

Nuclear fusion

Fusion Reaction Rates in Plasmas To utilize nuclear fusion for energy production, the fuel should be in the plasma state. In an ordinary state of matter, it is difficult to cause a number of fusion reactions. This is because most of the reactant's kinetic energies are quickly lost in the processes such as excitation and ionization of the constituent atoms, and dissociation of the molecules; the cross-sections for atomic and molecular processes are larger by several orders of magnitude than those for fusion reactions. These unfavorable processes can be avoided if the fuel is in the plasma state. In high-temperature plasmas, a certain fraction of the plasma ions can have energies high enough to overcome (penetrate) the Coulomb potential barrier.

In the Sun and other stars, the principal nuclear reactions begin with the conversion of hydrogen into deuterium [1]: $p + p \rightarrow D + e^+ + \nu_e$ (4.2 MeV) where p, D, e^+ , and ν_e denote proton, deuteron, positron, and electron neutrino, respectively. If the subsequent annihilation of the positron (e^+) with an ambient electron is added, the total energy release becomes 1.44 MeV. Anyway this first-step reaction occurs very rarely because it involves weak interaction (a proton changes to a neutron); its cross-section is immeasurably small (about 10^{-53} m^2 at 1 MeV, for example).

Variables

The reaction using ordinary hydrogen (p) is thus useless as an energy source on Earth. The main fuels for controlled fusion are the hydrogen isotopes, i.e., deuterium (D) and tritium (T).

The D-T reaction $D + T \rightarrow {}^4\text{He} + n$ (17.59 MeV) has advantages over other fusion reactions using hydrogen isotopes. The reaction Q-value (shown in the parentheses) is the largest of the reactions between hydrogen isotopes, and the cross-section at low energy is considerably large. This is because at energies below the height of Coulomb potential barrier B_1 , the D-T reaction predominantly proceeds via the formation of an excited state of compound ${}^5\text{He}$ nucleus, which gives a strong resonance in the cross-section (see Fig. 1.3 in Chap. 1). Deuterium occurs naturally in water with an abundance ratio of 0.015 %, but tritium is not available from natural sources, and therefore, one has to produce it in an artificial way.

The D-D reactions $D + D \rightarrow {}^3\text{He} + n$ (3.27 MeV) or $D + D \rightarrow {}^3\text{H} + p$ (3.03 MeV)

Ignition Condition and Requirement for Magnetic Confinement Fusion The essence of the controlled thermonuclear fusion is to confine the plasma of hydrogen isotopes for a long time so that the fusion reaction rate becomes large enough to generate the desired power. Two major schemes to achieve this goal are magnetic confinement fusion (MCF) and inertial confinement fusion (ICF). The basic principle of MCF is that in a magnetic field, charged particles move gyrating along the line of magnetic force. The transverse motions are nearly suppressed, and it is therefore possible to confine the plasma particles by using an appropriately designed magnetic field. The most established magnetic confinement device at present is tokamak. In this section, we derive a necessary condition for steady-state operation of MCF plasma on the basis of a simple power-balance model. The condition for ICF plasma is discussed in the next section. An excellent introduction to MCF is found in Stacey [3]. As for tokamak.

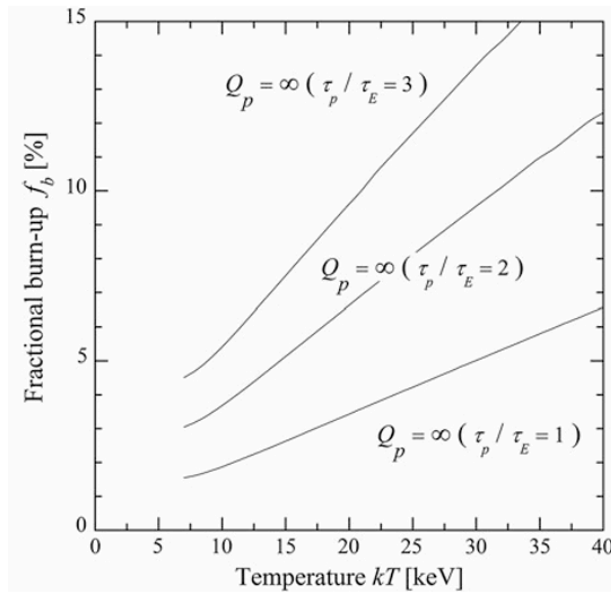
The power P_a and an external auxiliary heating power P_{aux} are delivered to the plasma to maintain the operating condition, compensating the power losses due to (1) electromagnetic radiation and (2) transport

across the magnetic field (i.e., thermal conduction and convection). An important measure here is the plasma fusion multiplication (or briefly the plasma Q-value) Q_p defined by $Q_p = P_{\text{fus}} / P_{\text{aux}}$ [4:23]

Example: The 'ignition' may be defined by a state that the temporal rate of increase in the internal energy (or temperature) of the hot spot is significant so that the burn wave propagates without any external heating. The rate of change in the internal energy per unit volume of the hot region is determined by the balance between the α -particle heating power P_α and loss powers due to the radiation (P_{br}), electron thermal conduction (P_C), and fuel expansion (P_W), that is $d/dt (3nkT) = P_\alpha - P_{\text{br}} - P_C - P_W$ [4:41]

Fractional Burn-up of Fuel in Core Plasma At the end of this chapter, we roughly estimate the fractional burn-up of DT fuel both in MCF and ICF schemes. First, let us consider MCF burning core plasmas. In this case, the fractional burn-up f_b is defined as the ratio of the fuel depletion rate due to fusion reactions to the rate of fuel injection into the core plasma region, that is $f_b = \text{depletion rate} / \text{injection rate} = 2 \Gamma_{\text{D}} / S_{\text{inj}}$ [4:41]. The factor '2' in the numerator accounts for the number of fuel particles lost per reaction. At steady state, the loss of fuel particles due to reactions and cross-field diffusion from the core is compensated by injection.

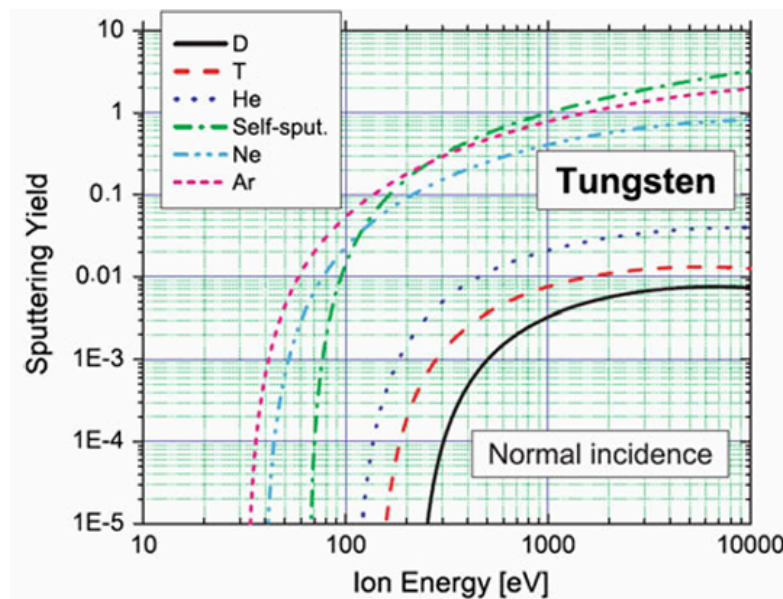
f_b for the case of $Q_p = \infty$ as a function of plasma temperature. The value of f_b increases with the temperature. Larger confinement time ratio τ_p/τ_E gives larger f_b . When $kT = 20$ keV (10 keV) and $\tau_p/\tau_E = 2$, for example, $f_b = 7\%$ (4%). If τ_p/τ_E were set to be unity, $f_b = 3\%$ (2%); almost the same f_b values were previously derived by Stacey [12], where the operating regime of D-T fusion plasma was discussed under the condition that $B = 10$ Wb/m², $b = 5\%$, and $\tau_p = \tau_E$. In a recent report [13]



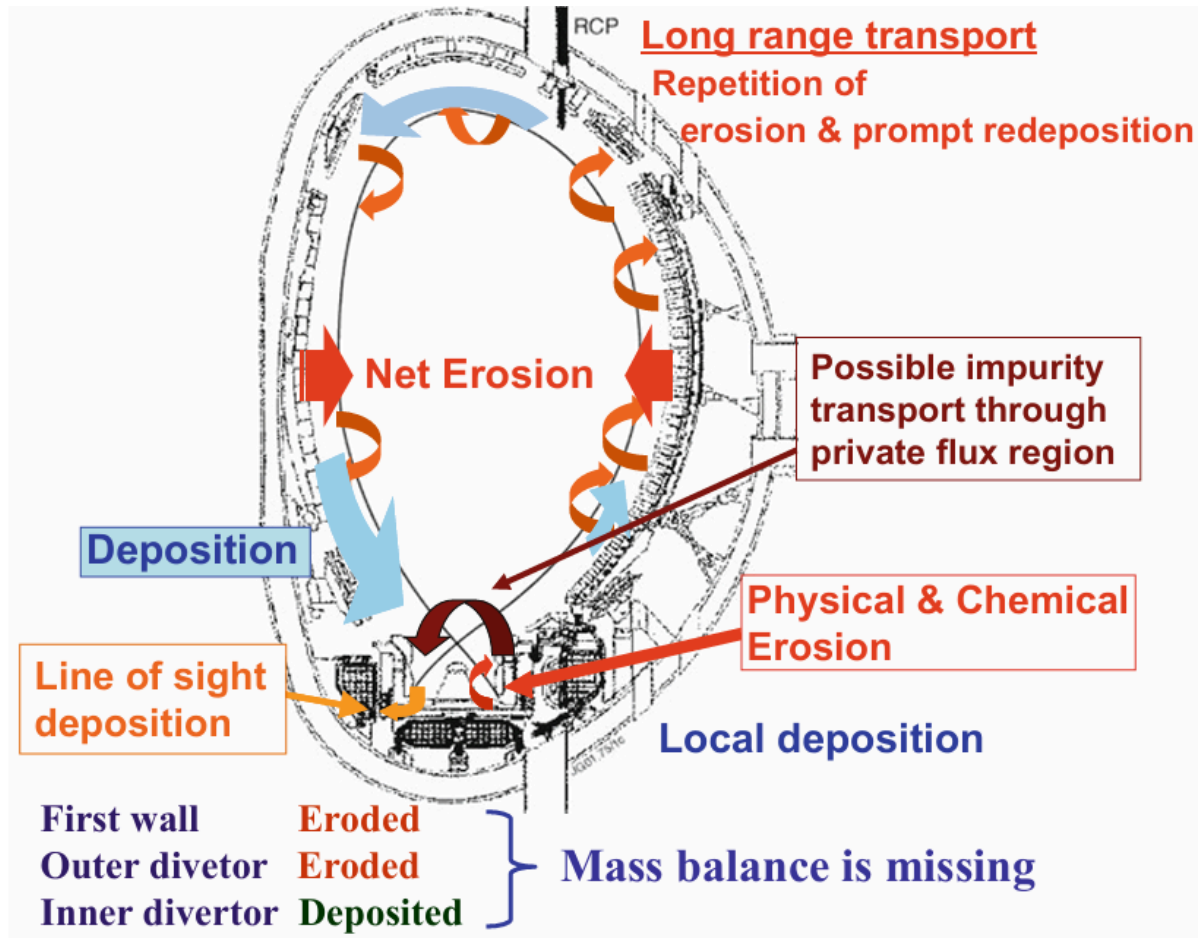
In reactor engineering studies, it may be usual to use the burning efficiency FB which is defined as the ratio of burned fuel to the throughput fuel. The relation between the fuel throughput (per unit time per unit volume) S_{thr} and our injection rate S_{inj} used in Eq. (4.41) is $S_{\text{thr}} = S_{\text{inj}} \eta_f$, where η_f is the fueling efficiency, the fraction of throughput fuel that gets to the core region. Thus, $FB = \eta_f f_b$ and $\eta_f < 1$. Although unknown at present, the fueling efficiency η_f is one of the important parameters for reactor system design. Actually, a

fusion reactor will be operated at $Q_p < \infty$, a state below self-ignition. Lower Q_p gives smaller f_b because the value of confinement parameter $n_s E$, appearing on the right-hand side of Eq. (4.43), becomes small with decreasing Q_p . Thus, in MCF, the burning efficiency would be less than 10 % even when the perfect fueling ($\eta_f = 1$) should be attained. Let us turn to the case of ICF fuel. We here suppose again a compressed DT plasma sphere which has uniform density q and temperature T at time $t = 0$, with a free boundary at radius R_f . The fractional burn-up of fuel f_b is then obtained from $f_b = \frac{1}{4} \frac{n_0 - n_{\text{seff}}}{n_0}$.

Plasma facing surfaces are exposed to energetic particles escaping from plasma as well as residual gas mostly composed of fuels (D and T). When the energy of the impinging particles exceeds the threshold energy to displace surface atoms, the surface atoms are sputtered to leave the surface, which is referred to as physical sputtering. The threshold energy is larger for heavier surface atoms, and sputtering yield is larger for heavier impinging particles. Since plasma always contains impurities such as carbon (C), oxygen (O), and helium (He) produced by D-T reactions, the physical sputtering by these impurities is significantly larger than that by fuel ions. Figure 5.1 shows sputtering yields of tungsten (W) [1] by hydrogen and some impurities, which is most likely to be used as the plasma facing surface of a fusion reactor.



Hydrocarbons, mainly methane, as the products of the chemical erosion of C, are emitted to plasma and ionized. But most of them are promptly redeposited by gyration in strong magnetic fields at the vicinity of the eroded area to make redeposited layers. (prompt redeposition). It should be noted that hydrogen concentration (in H/C atomic number ratio) in redeposited layers is different from the ratio of incident fluxes of H and C. Because hydrogen flux impinging to the surface $\propto \sqrt{m_H}$ is much larger than impinging carbon flux $\propto \sqrt{m_C}$, i.e., $\sqrt{m_H}/\sqrt{m_C} \approx 1/4$, the maximum H/C in stable hydrocarbons, most of incident hydrogen is reemitted. Accordingly, H/C in the redeposited layers is controlled by their temperature; the higher the temperature, the lower the H/C.



the general features of hydrogen recycling at PFM (metals) [7]. Energetic hydrogen ions and neutrals escaping from plasma impinge to PFS. Except directly reflected ones which are a few tens % of the impinging flux, the impinging fuel ions and neutrals are injected into the material within a certain depth referred to as projected range (varied depending on the incident energy). Most of the injected fuel particles diffuse back to the front (injected) surface (reemission), and remaining migrates or diffuses into be dissolved or trapped, and permeates to the back surface to be released as H₂ molecules.

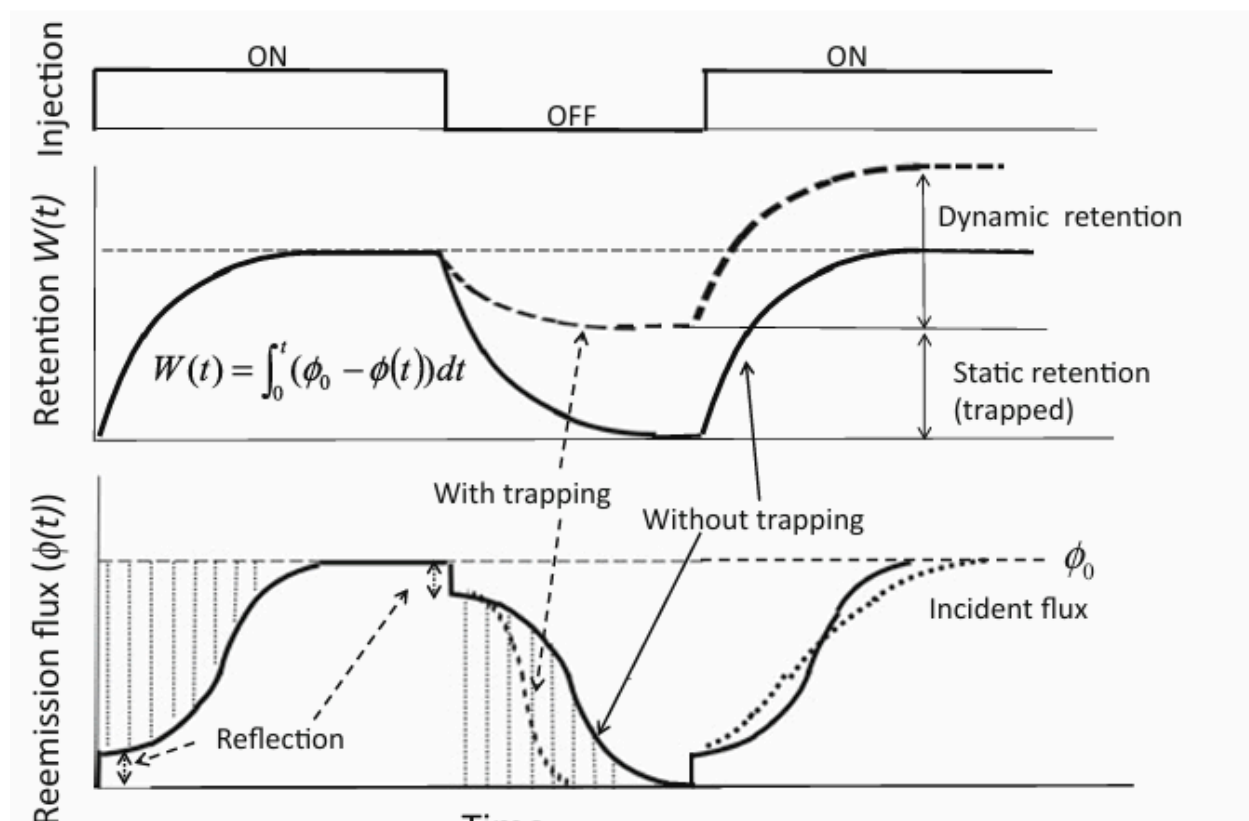
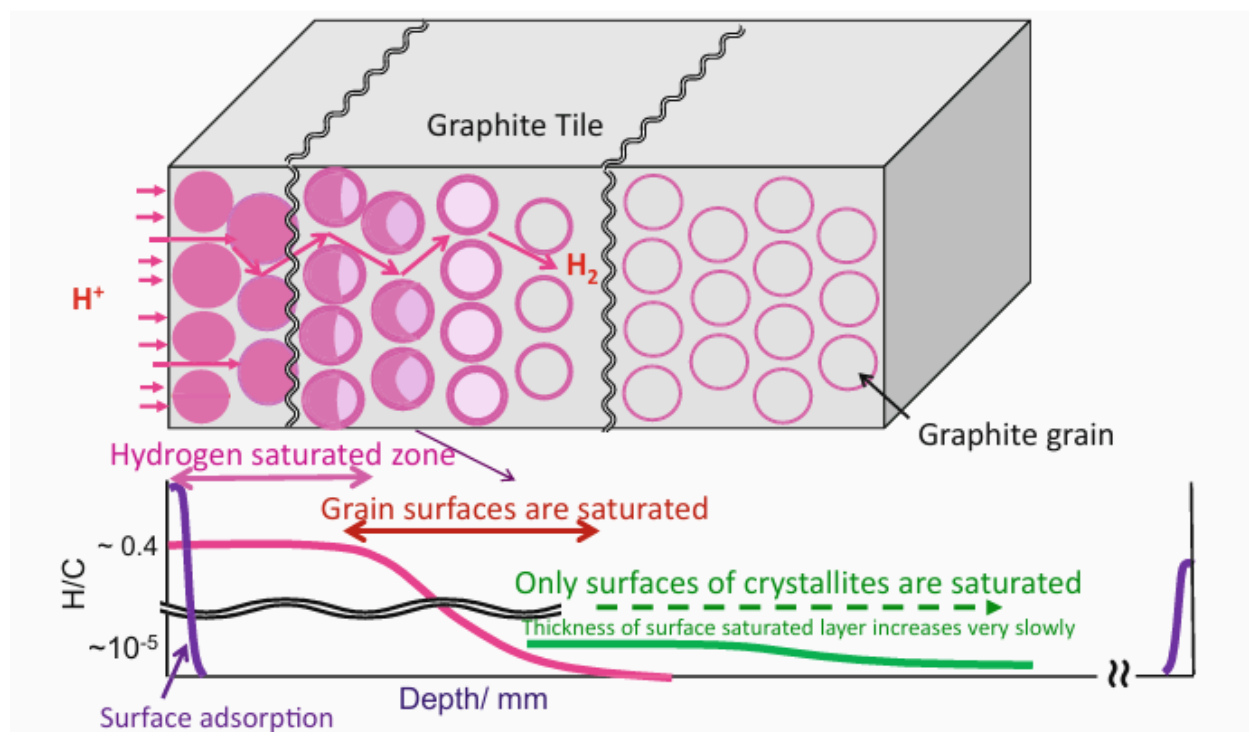
energetic fuel particle injection produces new defects in PFM, which can trap fuels subsequently injected, the true steady state is hardly attained. Nevertheless, the retention rate or difference between the injected flux and reemitted one becomes less and less toward the saturation. Hence, after a certain time of the injection, the reemitted flux becomes nearly constant equivalent to the incident flux. However, the integrated amount of the retained flux or the injected fluence becomes quite large. It is quite difficult to evaluate $W(t)$ accurately after the long time of plasma exposure. In principle, the integration of the flux balance Eq (5.1) gives the $W(t)$. However, the accuracy of the measurements of $I(t)$ only 2 to 3 digits does not allow the reliable evaluation of $W(t)$. As indicated in the figure, the total retention during the injection includes two components: “dynamic retention” and “static retention.” The former is directly connected to the fuel recycling and the later to the T inventory. The latter decreases with increasing temperature, because trapped fuels can be detrapped thermally. Irradiation of energetic ions and neutrons produces various defects such as interstitials and vacancies, their

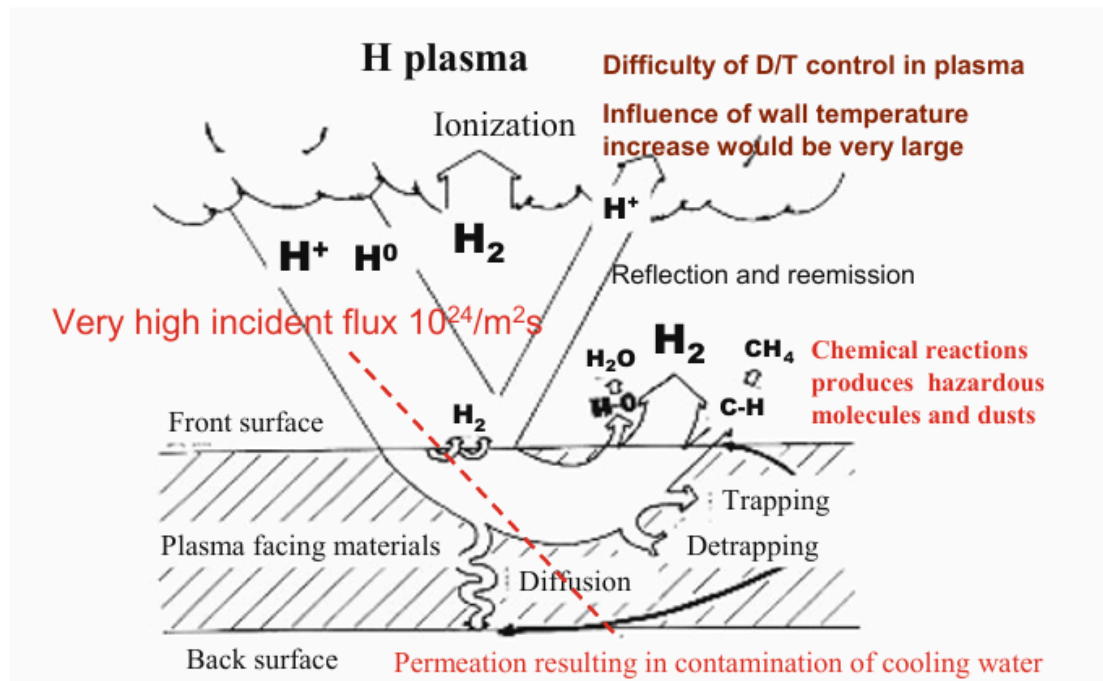
clusters or dislocation loops, and bubbles, which work as additional trapping sites to increase significantly the static retention or in-vessel T inventory, especially for W []

the reemission for carbon materials (C) includes methane resulting from chemical sputtering and causing significant surface recession (erosion). In addition, retention properties in C are quite different from those of metals. As shown in Fig. 5.5, a significant amount of injected fuels into the metals is released after the termination of the injection, i.e., the difference between the dynamic retention and the static retention is not large. In contrast, injected H in C is trapped near the projected range making C–H bond, and very small diffusivity in C inhibits the migration of H into the bulk, while their porous nature allows hydrogen molecules to penetrate deep through open pores, resulting in hydrogen profiles given in Fig. 5.6. This means that residual fuel gases in a reactor vessel can penetrate through the whole thickness of a carbon tile, resulting in all carbon grain surfaces being saturated with hydrogen.

Mechanism of H retention in carbon materials. Different from metals, the carbon materials are constructed of graphite like grain particles and fillers to be filtrated. H Migration of H impinging to them can be separated to two different schemes. One is directly impinging into the particles. But diffusion is too slow for H to penetrate deeper than its projected range. The other is penetration of H₂ molecules recombined at the particle surfaces deep inside through open pores among the particles.

hydrogen concentration exceeds the saturation concentration, H subsequently impinging is either recombined to be reemitted as H₂ molecules, or released making volatile hydrocarbons such as CH₄, which is the origin of the chemical sputtering. Furthermore, the hydrocarbons produced by the chemical sputtering enter into boundary plasma and impinge again to make redeposited carbon layers. Repetitive processes of erosion and deposition cause long-range transfer of carbon atoms, and as a whole, the first wall is mostly eroded and the inner divertor and plasma shadowed area are deposited as shown in Fig. 5.3. Redeposited carbon layers on the plasma shadowed area are saturated with H and D, which become the dominant in-vessel T inventory as discussed in the next section. Since any hydrocarbons are not stable at elevated temperatures, which is the reason for the reduction of chemical sputtering above around 800 K, the saturation concentration at elevated temperatures decreases appreciably and becomes a similar level to that of metals.





Hydrogen Retention and Carbon Deposition:

Tokamaks, and carbon tiles at the outer divertor area are eroded and those at the inner divertor area deposited by the eroded carbon. But materials balance between the erosion at the outer divertor and the deposition at the inner divertor is missing as shown in Fig. 5.3. The former is less than the latter, and the missing mass is likely compensated by erosion at the first wall of the main chamber, for which no systematic measurements have been made. The carbon redeposition occurs by repetitive processes of erosion and prompt redeposition of the eroded carbon as already discussed. In addition, there appears line-of-site deposition at remote areas from plasma, tile gaps or tile sides, and divertor opening for pumping. The deposition in tile gaps is much larger for surface-eroded tiles compared to that for surface-deposited tiles [16], which is the evidence of prompt redeposition of eroded materials. D is incorporated in the redeposited layers. But this is not due to simultaneous deposition (codeposition) of eroded carbon with D. The concentration of D in the redeposited layers is modified afterward. Generally, injecting D flux to PFM from plasma is significantly higher than that of impure carbon flux. Accordingly, most of the injected D is spontaneously reflected and/or reemitted and only part of the incoming D remains in the redeposited C layers with a saturation concentration of 0.4 in D/C at maximum.

JET MK-IIA (DTE): Deposition rate: 6.5×10^{20} C/s, Fuel retention rate: 5.8×10^{20} D-T/s (D/C=0.8), Fuel retention fraction: 0.17 (DTE1), 0.11 (DTE2); Remarks: T retention after non-mechanical cleaning, long-term outgassing and mechanical removal of accessible T deposit

JET MK-IIIB (DTE): Deposition rate: 4.3×10^{20} C/s, Fuel retention rate: 1.25×10^{20} D-T/s (D/C=0.3), Fuel retention fraction: 0.03; Remarks: D retention from postmortem analysis

TFTR (DT Campaign): Fuel retention fraction: 0.16

ASDEX Upgrade (DD): Deposition rate: 3.5×10^{20} C/s, Fuel retention rate: 0.035 D-T/s, Fuel retention fraction: 0.1; Remarks: D retention from postmortem analysis and fuel balance

TEXTOR (DD): Deposition rate: 2.5×10^{20} C/s, Fuel retention rate: 1.6×10^{19} D-T/s, Fuel retention fraction: 0.08; Remarks: D retention from postmortem analysis

Tore Supra (DD): Deposition rate: 2.5×10^{20} C/s, Fuel retention rate: 0.5 D-T/s; Remarks: D retention from fuel balance in dedicated long-pulse discharges

JT-60U (DD): Deposition rate: $3 \times 6 \times 10^{20}$ C/s (plasma facing area only), Fuel retention rate: 5.3×10^{18} D-T/s (D/C=0.02), Fuel retention fraction: 0.0 (for saturated wall); Remarks: Wall saturation appeared at 573K operation, DDD discharges with DNBI heating

H, D, and T in a JT-60 carbon tiles exposed to DD discharges and HH discharges subsequently made for T removal. By the HH discharges, D retained during the DD discharges was isotopically replaced as shown in the top. Note that T concentration is several orders of magnitude less than H and D concentrations.

Hydrogen dissolves in the form of either molecules and atoms or ions, depending on the type of the material. The molecular dissolution is observed for polymers, whereas dissolution in the forms of atoms or ions is typical for metals and dense ceramics. The form of hydrogen dissolution in a material can be understood from the dependence of the concentration of dissolved hydrogen CH [mol m⁻³] on the hydrogen gas pressure P [Pa] under the equilibrium conditions: $CH = KSP$ (Henry's law), if hydrogen dissolves in the molecular form; and $CH = KSP^{0.5}$ (Sieverts' law [1]), if hydrogen dissolves in the form of atoms. Here, KS is the solubility [mol m⁻³ Pa⁻¹ or mol m⁻³ Pa^{-0.5}]. Because metals and ceramics are more important for tritium confinement and separation, the attention is focused on hydrogen permeation.

This part is characterized by an asymmetric blue wing with respect to the cold component. Although the light is emitted from the bulk ions, this asymmetry is principally due to the favoring of charge transfer to plasma deuterons commoving with beam because of the rapid fall of the charge exchange cross sections for relative velocity $v > 1.5 v_{Bhor}$ (v_{Bhor} is the Bohr orbital speed = 25 keV/amu). "C" is characterized by Doppler-shifted emission from the beam deuterons. Three components (C1, C2, C3) are associated with the full, half, and third energy components. For H, D-mixed plasma CX spectrum has been analyzed in the TEXTOR H-beam injection experiment [30]

Plasma parameters

In the burning plasma, the fueling into the core region is considered to be done by fast neutral beams. Different from the passive Balmer- α emission (originated from the electron impact excitation), which is restricted with the emission from the edge, the neutral beam has diagnostic potential to measure intense Balmer- α 198 H. Zushi emission in the core. The Da-ACX line associated with the fast neutrals is emitted in plasma by the following active charge exchange process, D0 beam pDp plasma ! Dp beam $pD0$ plasma ! Da ACX $\delta 8:32p$ Here D0 plasma means the excited state of D atom. The active CX photon flux $/a$ -ACX is given by $/a$ ACX $\frac{1}{4} 1 4pndnbeam$ rv h $icxDl$; $\delta 8:33p$ where Dl is the path length and bracket must be calculated by taking the velocity distribution functions for bulk ions and beam particles into account.

This emission line is overlaid on the emission due to the electron impact excitation and passive charge exchange excitation with the neutral D0 recycled from the wall. The former and latter are named "cold" and "warm" components, depending on their radial location. D0 pe !D0 plasma pe ! Da thermal D0 recycle p Dp

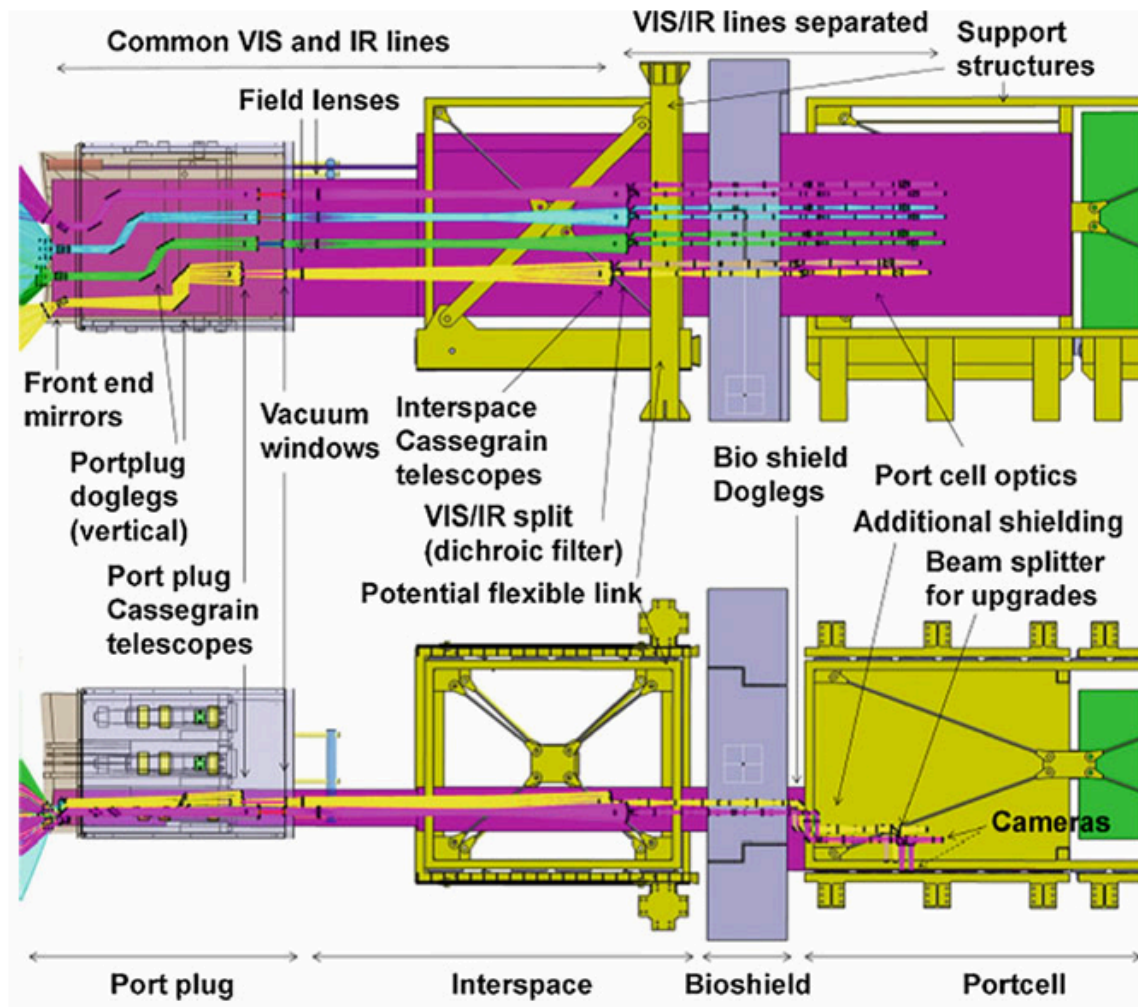
plasma ! Dp recycle pD0 plasma ! Da PCX 08:34:1P 08:34:2P In order to obtain the ACX component above two spectra must be subtracted from the observed spectrum.

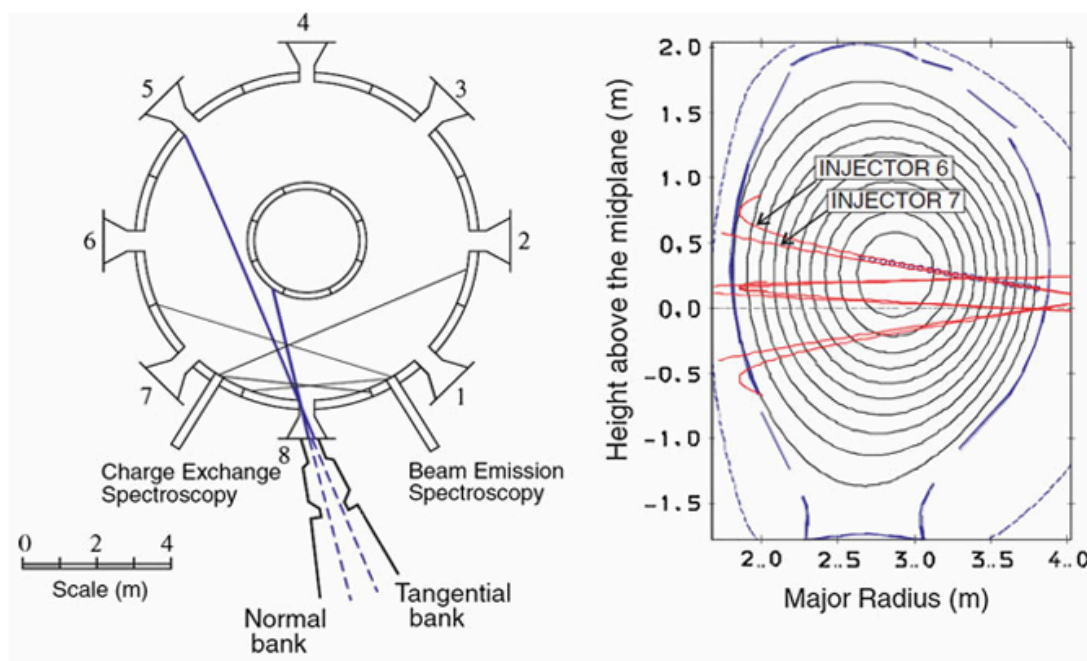
The beam Balmer- α emission Da beam via the following three collisional processes can be also observed in the vicinity of Balmer- α line [27]. D0 beam pDp plasma ! D0 beam pDp plasma ! Da beam; D0 beam pApZ plasma ! D0 beam pApZ plasma ! Da beam D0 beam pe ! D0 beam pe ! Da beam 08:35:1P 08:35:2P 08:35:3P These processes are dominated by collisional excitation of the beam atoms with fuel deuterons, fully stripped impurities and electrons. Line emissions caused by the neutral beams are Doppler-shifted depending on the velocity of the injected particles and on the angle between the beams and the viewing lines. The beams intersect the magnetic field lines at some angle and a strong magnetic field is therefore experienced by the neutrals in their center of mass frame.

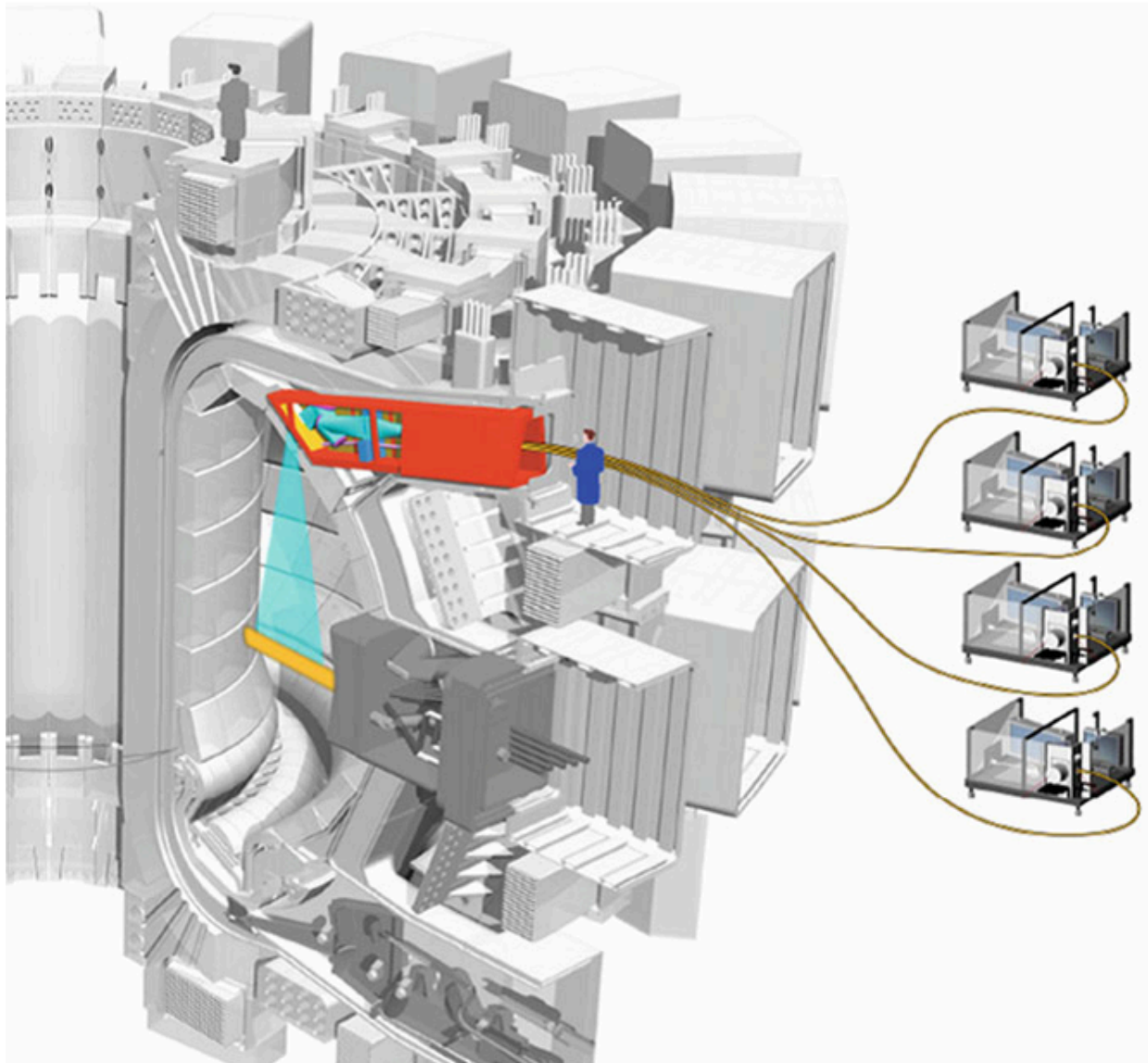
The vbeam BLorentz electric field perturbation causes the Da-beam line (motional Stark emission, MSE) to split into 15 Stark components ($0r, \pm 1r, \pm 2p, \pm 3p, \pm 4p, \pm 5r, \pm 6r, \pm 7p$), 9 of which are usually strong enough to be observed. The beam consists of three energy fractions ($E_0, E_0/2$ and $E_0/3$), corresponding to D⁺, D2⁺, D3⁺ in the positive-ion source of the beam injectors.

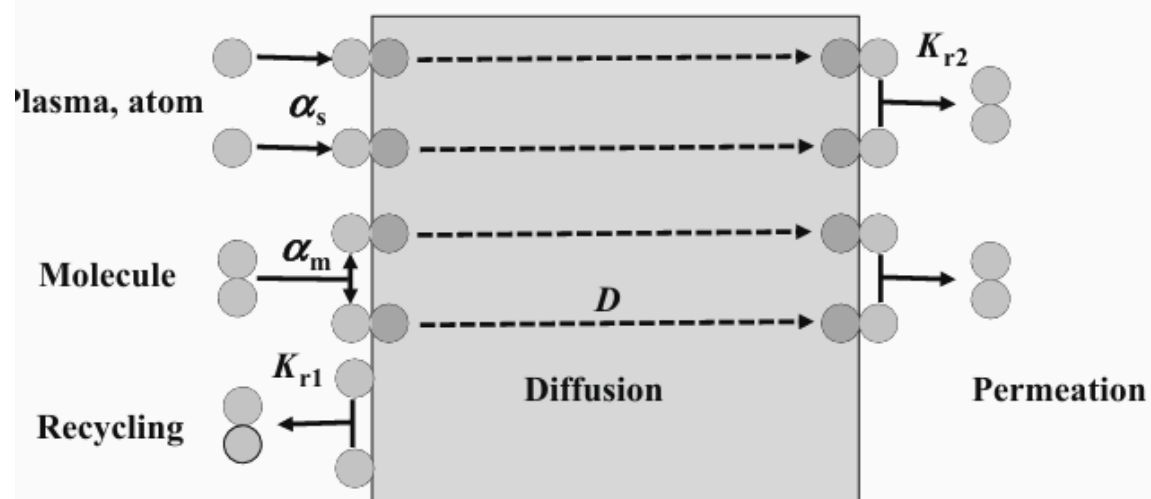
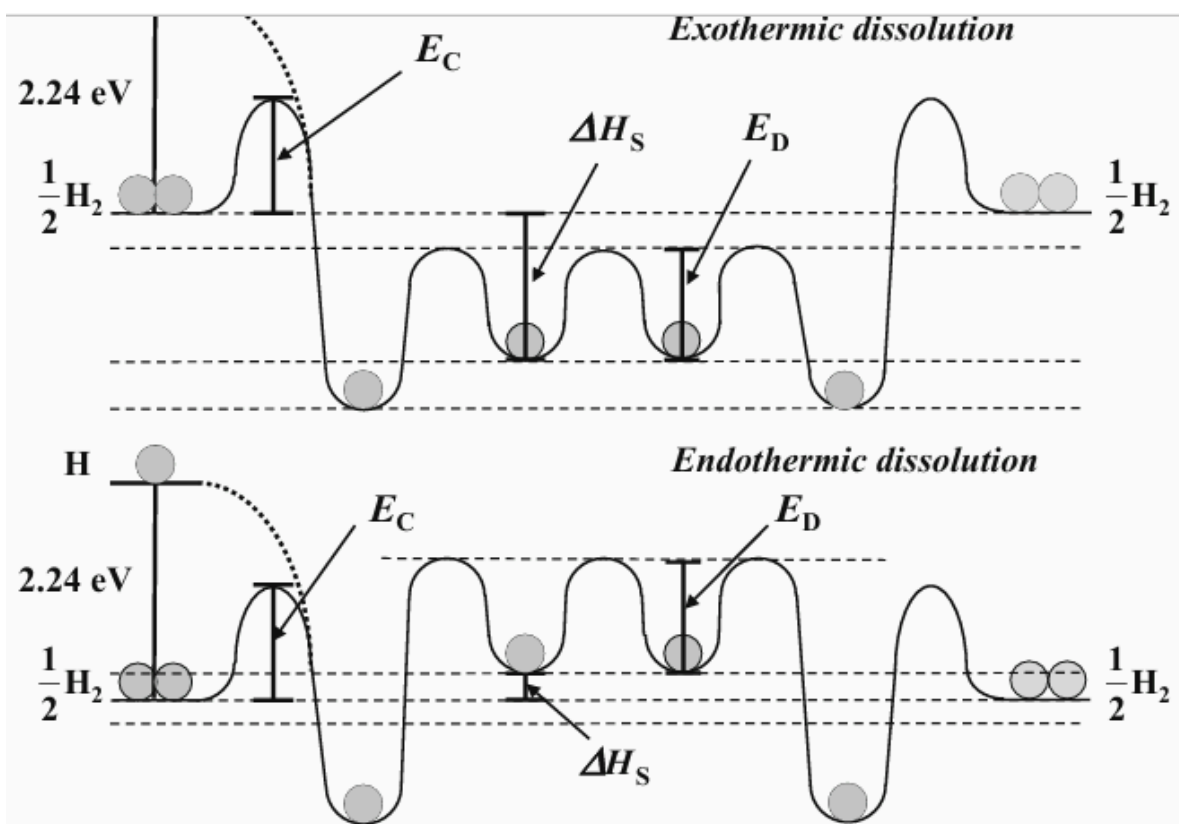
H₂, D₂, HD is introduced [16].

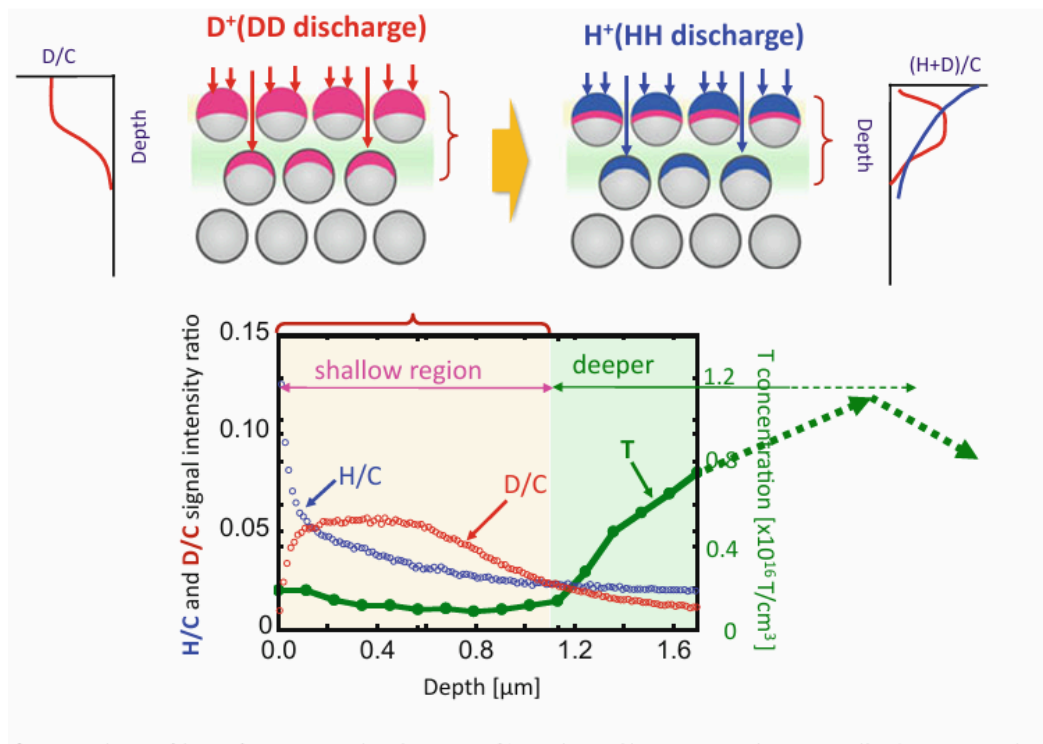
Molecules: Each concentration of isotopologues is described as follows: CH₂ CD $\delta P/4$ 1 1p CD K 1 1 CD CHD CD K₂ p CD $\delta P/4$ 1 1p1 CD CD CD₂ CD K 2 K₁ p CD 2 1 CD 1 CD 1 K₁ 1 K₂ ; $\delta P/4$ 1 1p1 CD CD K₁ p CD 1 CD K₂ ; ; 08:31P Here the surface recombination coefficients k_{H_2} , k_{HD} , k_{D_2} , and equilibrium constants $K_1 = k_{H_2}/k_{D_2}$ and $K_2 = k_{HD}/k_{D_2}$ are used for a H₂, HD, and D₂ reaction system. When $K_1 = K_2 = 1$, the isotopologues concentration is simply determined.









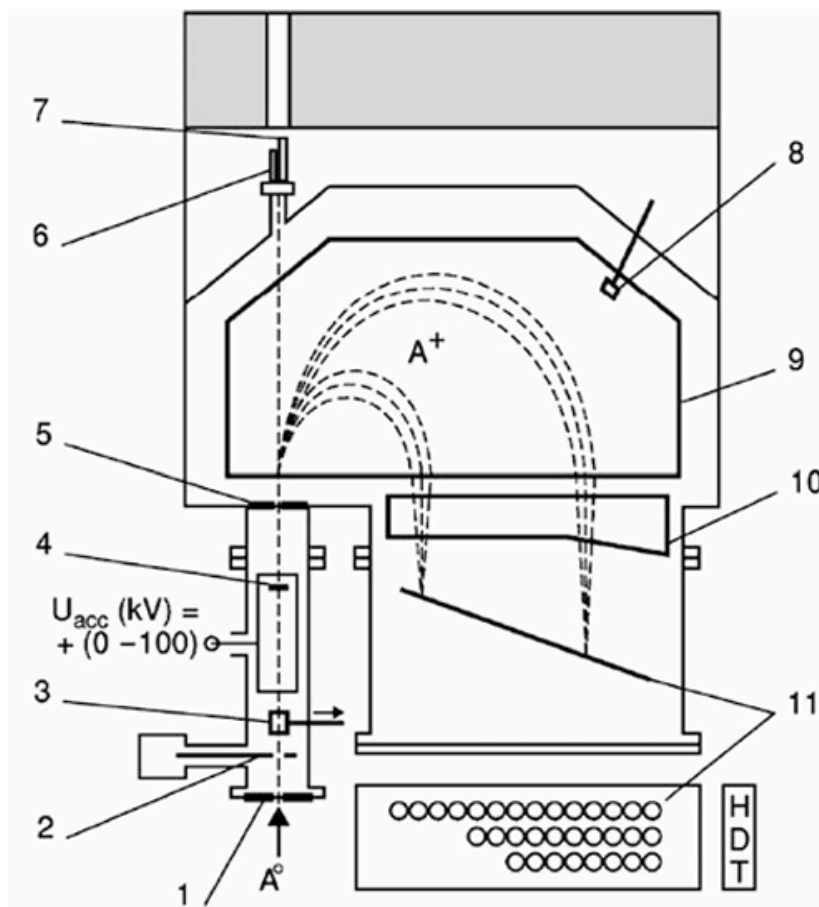
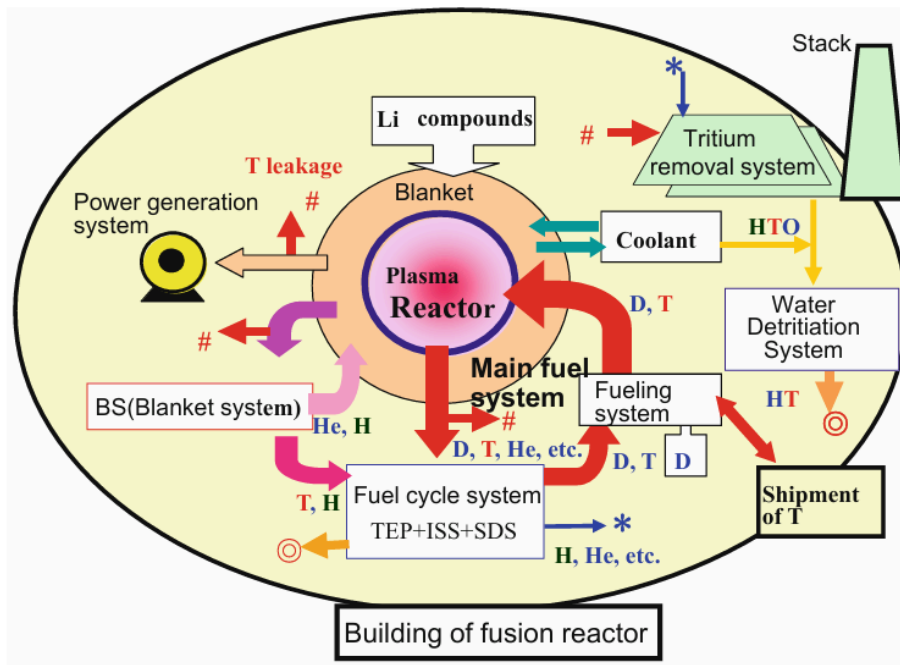


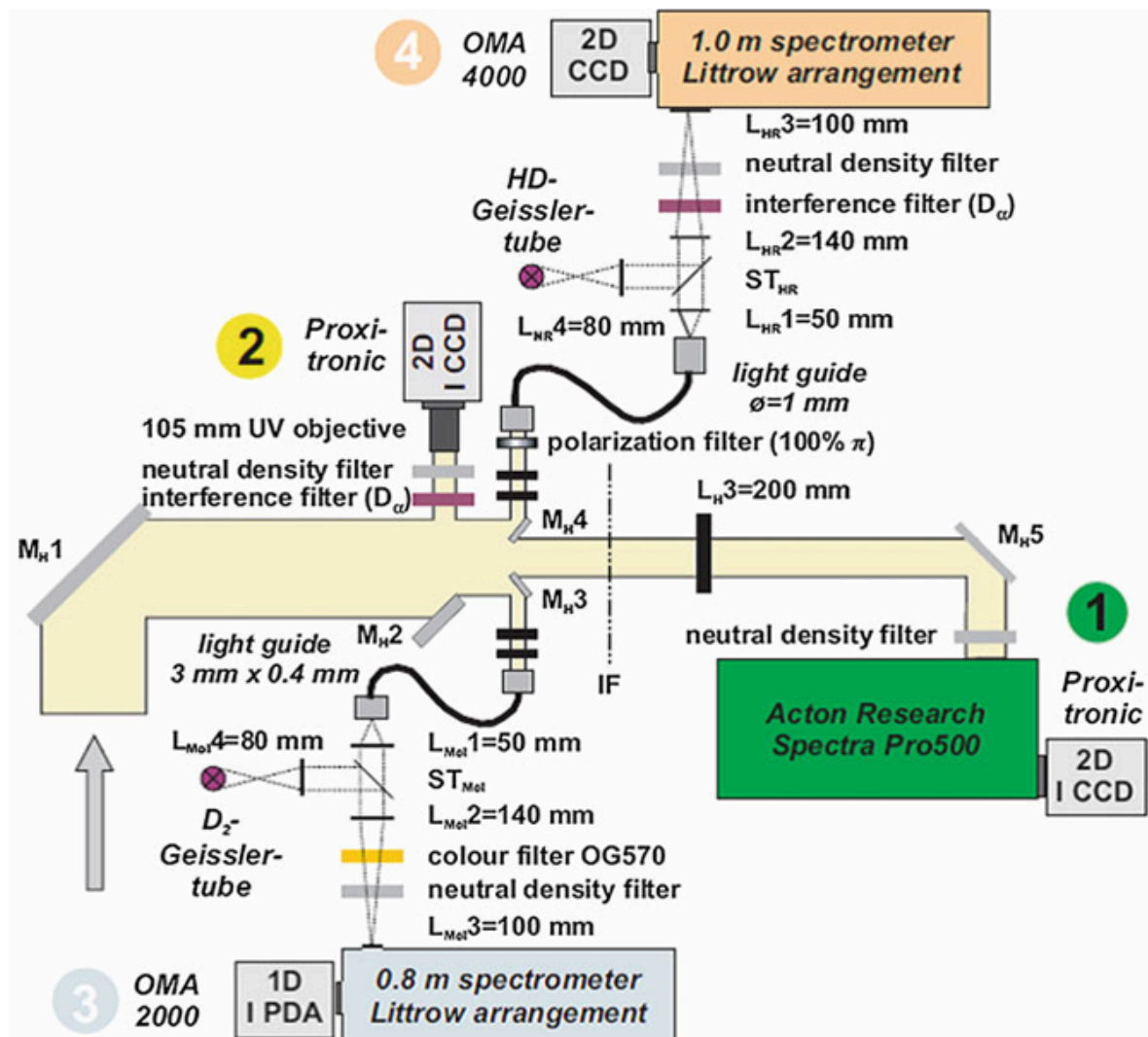
Example: In the 1–10 keV energy range, the two terms inside the square brackets do not depend on the isotope chosen. Thus, for the isotope density ratio, one may write $n_H/n_D = \frac{1}{2} \left(\frac{H}{D} \right)^2 \frac{1}{\delta}$ where $\delta = \frac{m_H}{m_D}$ is a correction factor for mass difference at the given energy. Since NPA can analyze energy spectra of fast neutrals (H_0, D_0 , and T_0) escaping from the plasma and these atoms of different energies come from different radial positions inside the plasma, precious information about the isotope composition profile is contained in the NPA-detected signal. Method and instruments: Figure 8.14 shows an NPA [called ISotope SEPARATOR (ISEP)] layout used in JET [13]. It consists of three main chambers such as acceleration, magnet, and detection. The acceleration chamber consists of an input aperture, a collimator slit mechanism, a removable calibration aid, a thin carbon stripping foil supported on nickel mesh, and an output aperture. Elements of the magnet and detector chambers are a light emission diode for detector testing, optical laser for alignment, a Hall probe, the magnet that gives a nonuniform field, an electrostatic condenser that gives a nonuniform electric field, and a detector array. A neutral atom with mass A enters into the entrance slit (2 mm u) of the acceleration chamber. The positive electrode of the accelerator consists of a hollow polished stainless steel cylinder with 8-mm apertures on the axis at both ends. The secondary ion A^+ can be created through the thickness of 30 nm and diameter of 12 mm u carbon stripping foil mounted inside the cylindrical electrode close to the exit end. A thin nickel mesh with 90 % transmission supports the foil. Acceleration voltage of $U_{acc} = +0.1$ MV is used.

the main fuel system is a combination of chemical processes. One of the significant features of the system is that radioactivity of T does not allow its leakage and requires recovery of the leaked T . For T safety, a series of T -removal systems is prepared to confine T in a fusion reactor facility. All the components in T -processing systems should have a leak tight structure to avoid T leakage as low as reasonably achievable (ALARA). Even if T was released into a fusion reactor building by an accident or by a miss-operation, the amount of T

released to the environment should be controlled to be less than a regulation value and should be decreased to be ALARA. Some maintenance works are required for T-contaminated components, and these components would be dismantled. Some amount of T would be released through the maintenance works. To confine T, the maintenance works would be carried out in a hot cell, whose atmosphere is maintained at a negative pressure. The atmosphere gas in the hot cell is further circulated through the T-removal system. In the T-removal system, T released into the atmosphere of the hot cell is oxidized by a catalyst reactor and removed by a molecular sieve dryer or a scrubber column. A regeneration process of the molecular sieve dryer produces tritiated water.

A detritiation system consisting of a scrubber and molecular sieve dryer is essential. For a fusion reactor, when T level in coolant water exceeds the regulation level owing to T permeation, the coolant water should be also processed by the water detritiation system as shown in Fig. 6.1. T recovered by the water detritiation system is sent to the fuel cycle system to reuse as fuel. The detritiated water is exhausted to the environment. ITER is the first device which equips the abovementioned main fuel system [1]. In some previous plasma devices carrying out T experiments such as TFTR and JET, T fueled into their plasmas was not recycled, while ITER will be the first system to reuse fueled T. Furthermore, the first test trial of recovery of bred T in the blanket will be done in its technical phase. For instance, to obtain 1 GWe output from a fusion reactor, the amount of T fueled into the reactor (throughput) will be 10 kg/day in the case where the conversion factor of energy from heat to electricity is 1/3 and a burning efficiency of T is 4 %. We must establish the fueling system with such high T throughput in a fusion reactor. A series of demonstration tests of a test blanket module is a main subject in ITER for a next-generation machine and a DEMO reactor.





Fuel Injection System DT fueling into burning plasma is one of the key issues for stable fusion reactor operation. In the case of magnetic confinement, there are two types of techniques depending on the energy of fueling particles. One is the high-energy particle injection, such as neutral beam injection (NBI), which is also used for plasma heating. Recently, compact toroidal injection [3] is also proposed using small plasma of fuel, instead of NB. The other is ambient or lower temperature particle injection, such as gas puffing or pellet injection. For any fueling in magnetically confined fusion, it is a main issue how to fuel into the core plasma without cooling down the core plasma. Inertially confined fusion uses a spherical solid target. The fuel gas of D–T is condensed into the spherical porous polycarbonate form. In ITER, about 300 mol/h of D–T (50–50 %) gas is charged into the plasma. About 20 % D–T is charged by the high-temperature particle injection such as NBI, 25 % D–T is charged by the pellet injector, and the gas puffing supplies the rest of D–T. For a DEMO reactor, these percentages will be modified to obtain maximum burning efficiency. (1) Neutral Beam Injection This technique consists of collisional heating of plasma particles by injected high-energy neutral

particles. The technique is also used for fueling into the core plasma. In a neutral beam injection (NBI) system, fuel particles are first ionized and accelerated, and then neutralized to inject through the strong magnetic field of plasma. Either positive or negative ions can be used and they have to be accelerated to >1 MeV before the neutralization. To get higher efficiency in the neutralization, negative ions are mainly used. In the case of ITER (0.5GWth), for example, 40 A of negative deuteron beam is required to accelerate to 1 MeV, so that a few $10\text{ cm}^3(\text{stp})/\text{s}$ of deuterium is injected if neutralization efficiency is about 60 %.

(2) Compact toroidal injection [3] This technique is an injection method of small fuel plasma produced outside of the reactor core with high speed of a few 100 km/s. Because the fuel plasma can be injected close to the center of the core plasma, it is expected to get high fusion reaction efficiency.

(3) Gas puffing This is the most popular fueling technique with injection of fuel gas through high-speed electromagnetic valves (piezo valves) with response time of less than 1 s. In order to supply the fuel gas uniformly into the vacuum vessel, several gas-puffing ports with the piezo valves are installed.

(4) Pellet injection [4] 6 Tritium Fueling System 123 This technique is an injection of solid pellets of fuels. First, the pellets are made by pushing out solidified deuterium and/or tritium through piston or screw from the cylinder cooled by liquid He followed by cutting to be an adequate size. Then the pellets are accelerated by either centrifuge, gas gun, or rail gun methods. The centrifuge method can inject a few mm pellet with velocity of 1 km/s by a few 10 Hz, using high-speed rotated arm with high reliability. The gas gun, using 10 MPa of hydrogen or He, is demonstrated a few km/s of pellet velocity. Theoretically, the rail gun would inject the pellet with higher velocity than other methods.

6.2.1.2 Vacuum Pumping System

The pumping technology is very important to maintain fusion reactions by exhausting fuel mixture and transferring them to a T-processing plant. In a magnetic fusion reactor, R&D issues are to develop pumping systems to tolerate strong magnetic and high radiation fields, and to attain large pumping speed of about 300 mol/h of D–T fuel gas from the vacuum chamber as described in the previous section. Characteristics of major possible pumps are summarized as follows.

(1) Turbo molecular pump [5] This pump compresses gas molecules by a high-speed rotor and exhausts them to the downstream. Continuous operation of the pump is achievable. However, there is a concern on reduction of rotational speed of a metallic rotor in the strong magnetic field by eddy current. To avoid the effect of the magnetic field, recently, a ceramic rotor using SiN₄ has been developed. Moreover, gas-bearing and gas turbine rotation are selected as alternatives of magnetic-bearing and electric motor rotation, respectively, which promise more reliable performances in the strong magnetic field. In order to fabricate a pump with larger pumping capacity, a larger ceramic rotor is required. Progress of ceramic material technology is awaited.

(2) Cryosorption pump This pump evacuates gas molecules by sorption on the cryopanel cooled at about 4 K. Since the pump has no mechanically working parts, it is quite beneficial to use in strong magnetic field. Because of limited capacity in the sorption of the cryopanel, however, its periodical regeneration by thermal desorption of the absorbed gases is required. This does not allow its continuous operation but forces its batch operation. Owing to its operational ability under the strong magnetic field, ITER selects a series of cryopumps with periodic switching operations.

(3) Metal jet diffusion pump [5] In an inertially confined fusion reactor, it is quite important to ensure a stable operation of their evacuation pumps under vapors evaporated from liquid breeder covering the first wall, such as Li and LiPb. A metal jet diffusion pump using liq. Pb 124 T. Yamanishi has been investigated for operation in such circumstance. The pump has no mechanical working parts and is compatible with metal vapor and even dust. Its structure is very simple and allows high-temperature operation different from an oil diffusion pump. Scale-up demonstration is a further issue.

(5) Roughing pump All pumps except the cryopump require roughing pumps. To have capability to handle T, oil-free pumps are favorable. This is because tritiated oil would be produced as waste by easy isotopic replacement of H in the oil by T; it is not easy task to measure the T concentration in the oil. Pumps of scroll and reciprocating types without usage of the oil are available [6]